

Two-photon processes $\gamma\gamma \rightarrow \pi^+\pi^-$, K^+K^- in the modified perturbative QCD approach

Cong Wang^{1,*}, Jun-Kang He^{1,†} and Ming-Zhen Zhou^{2,‡}

¹*Institute of Particle Physics and Key Laboratory of Quark and Lepton Physics (MOE),
Central China Normal University, Wuhan, Hubei 430079, P. R. China*

²*School of Physical Science and Technology, Southwest University, Chongqing 400715, P. R. China*

As one of the simplest hadronic processes, $\gamma\gamma \rightarrow \pi^+\pi^-$, K^+K^- reactions could be a testing ground for our understanding of hadronic dynamics, and will be studied with high precision at Belle-II in the near future. In this paper, we revisit these processes in the modified perturbative QCD approach, in which transverse degrees of freedom as well as Sudakov suppression are taken into account. The twist-2 and twist-3 light-cone wave functions of pion and kaon mesons are used as the candidate forms for the nonperturbative dynamical inputs. It is shown that both the intrinsic transverse momentum and the twist-3 corrections can give sizable contributions to the cross sections at the intermediate energy region and should be kept for a better understanding of the two-photon processes.

PACS numbers: 12.38.Bx, 12.39.St, 13.60.Le, 13.66.Bc

I. INTRODUCTION

A meaningful and historic subject of the perturbative QCD, which has received considerable attention in the past few decades, is the study of the exclusive processes at large momentum transfer. The founders of this theory are Efremov and Radyushkin [1] and, independently, Brodsky and Lepage [2, 3]. They point out that the exclusive processes at large momentum transfer Q can be factorized into perturbatively calculable short-distance part and long-distance hadronic wave functions. Although there is general agreement that perturbative QCD is able to make successful predictions for the exclusive processes at asymptotic limit ($Q \rightarrow \infty$), the applicability of perturbative QCD to these processes at experimentally available Q region has been developed in controversy.

In the field of exclusive processes [2–4], two-photon processes [5–7] are of special interests since they can provide particularly suitable tests for QCD. Due to the initial states are simple and controllable, with strong interactions only in the final states, these characteristics simplify the analysis of the processes. In recent years, theorists have made many efforts to search the particular ones $\gamma\gamma \rightarrow \pi^+\pi^-$, K^+K^- by using a variety of theories, such as the perturbative QCD approach [8–11], the modified perturbative QCD approach [12–14], the handbag model [15–17] and the soft collinear effective theory [18]. In the experimental aspect, experimenters have measured the production cross sections of charged- [19–22] and neutral-pion pairs [23, 24] and, charged- [19–21, 25] and neutral-kaon pairs [26, 27]. Up to now, there is still an order of magnitude gap between the theoretical predictions and the experimental data of the cross sections.

In contrast to our previous work [28], we will employ the modified perturbative QCD approach based on k_T factorization instead of the collinear approximation. This method is proposed by Serman and his collaborators [29, 30] and its main idea is to retain the intrinsic transverse hadronic structure and incorporate the gluonic radiative corrections in the form of Sudakov factor, see Ref. [31] for more detailed discussion. The improved theoretical scheme was widely adapted in the studies of pion electromagnetic form factor [30, 32–34], P -wave quarkonium decays [35] and exclusive B decays [36, 37]. On the other hand, a general view is that the higher twist contributions are suppressed by the factor $1/Q^2$, however there are also theoretical works [33, 37, 38] confirmed that the twist-3 contributions are comparable with and even larger than the twist-2 contributions at currently accessible energies. Further studies in space- and time-like electromagnetic pion [39] and kaon [40] form factors also show the dominance of the higher twist contributions at low- and moderate-energies. As is known, the calculations for the higher twist contributions are much more difficult than that for the leading twist since the end-point singularity becomes more serious. The advantages of the modified perturbative QCD approach is that not only the soft end-point regions are strongly suppressed but also the large logarithms and double logarithms from higher-order corrections are effectively avoided. Because of that, the perturbative QCD calculation becomes self-consistent, even for momentum transfers as low as a few GeV region, and shows the dominance in the form factors and cross sections.

The purpose of this work is to reexamine the twist-3 contributions to the two-photon processes $\gamma\gamma \rightarrow \pi^+\pi^-$, K^+K^- in the framework of modified perturbative QCD approach. Comparing with the collinear approximation, the modified perturbative approach has some major improvements: First, both the intrinsic transverse momentum dependence of hadronic wave functions and that of hard kernels are included. The intrinsic k_T -dependence of the wave function substantially suppresses the contribution

* Electronic address: wangj@mails.cnu.edu.cn

† Electronic address: hejk@mails.cnu.edu.cn

‡ Electronic address: zhousm@swu.edu.cn

from the dangerous soft end-point regions. Second, the Sudakov resummation [30] and the threshold resummation [38] effects for pion and kaon mesons are taken into account. The large double logarithms $\ln^2 k_T$ and $\ln^2 x$ from higher-order loop correction are organized into the Sudakov factor $\exp[-S]$ and threshold factor S_t . The factor $\exp[-S]$ falls off quickly in large b region and the factor S_t vanishes at the end point $x \rightarrow 0, 1$, thus suppress the long-distance contribution and end-point singularity. Third, the scales of the coupling constant α_s are chosen to be momentum-fraction dependent in order to avoid large logarithms from higher-order perturbative QCD corrections. It is found that the cross sections for $\gamma\gamma \rightarrow \pi^+\pi^-, K^+K^-$ with twist-3 corrections at moderate energies in the modified perturbative QCD approach based on k_T factorization theorem are consistent with currently available experimental data [19–21].

This paper is organized as follows: In Sect. II, the related conventions to these processes are introduced at first, next the twist-2 and twist-3 light-cone wave functions are described briefly, then we perform the modified perturbative QCD calculation and the formulas of the hard kernels with twist-3 contributions are presented. The numerical analysis and discussion are given in Sect. III. The last section contains the conclusion and work towards. The expression of the Sudakov function can be found in Appendix.

II. PERTURBATIVE QCD CALCULATION

A. Kinematics and conventions

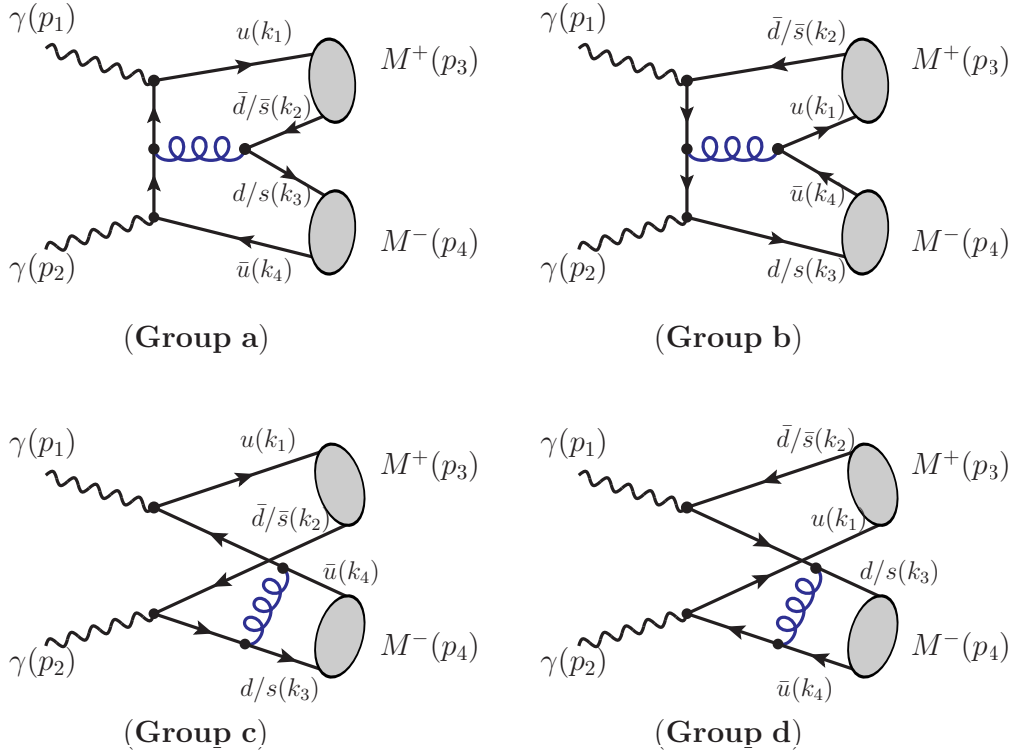


FIG. 1. Four basic Feynman diagrams for $\gamma\gamma \rightarrow M^+M^-$ ($M = \pi, K$). The total number of tree level diagrams in groups a, b, c , and d are 6, 6, 4, and 4, respectively. The grouping is based on the virtualities of the internal gluon.

We consider the simplest hadronic processes, $\gamma_1(p_1, \varepsilon_1^{\lambda_1})\gamma_2(p_2, \varepsilon_2^{\lambda_2}) \rightarrow M^+(p_3)M^-(p_4)$ ($M = \pi, K$), where the incoming photons are real with momenta p_1, p_2 and polarization vectors $\varepsilon_1^{\lambda_1}, \varepsilon_2^{\lambda_2}$ with the photon helicities $\lambda_1, \lambda_2 = \pm 1$, M denotes the outgoing pseudoscalar mesons with momenta p_3, p_4 . The contributions to the $\gamma\gamma \rightarrow (q\bar{q}) + (q\bar{q})$ amplitude arise from 20 tree-level Feynman diagrams, which can be grouped together into four basic types (a, b, c and d) based on the virtualities of the internal gluon. We depict the four basic Feynman diagrams in Fig. 1. The remaining diagrams arise from permutations of the gluon and quark lines.

For convenience, the amplitude is calculated in the center-of-momentum frame, with the final mesons momenta along the z -axis. θ is the scattering angle and Q denotes the collision energy. In the light-cone coordinate, a momentum A^μ has the form $A^\mu = (A^+, A^-, \mathbf{A}_\perp)$ with $A^\pm = A^0 \pm A^3$ and $\mathbf{A}_\perp = (A^1, A^2)$, the scalar product is defined as $A \cdot B = \frac{1}{2}(A^+B^- + A^-B^+) -$

$\mathbf{A}_\perp \mathbf{B}_\perp$. Under these conventions, the momenta can be written as

$$\begin{aligned} p_1 &= (2\omega c^2, 2\omega s^2, \mathbf{p}), & p_2 &= (2\omega s^2, 2\omega c^2, -\mathbf{p}), \\ p_3 &= (2\omega, 0, \mathbf{0}_\perp), & p_4 &= (0, 2\omega, \mathbf{0}_\perp), \end{aligned} \quad (1)$$

with $\omega = \frac{Q}{2}$, $s = \sin \frac{\theta}{2}$, $c = \cos \frac{\theta}{2}$ and $\mathbf{p} = (2\omega sc, 0)$, for simplicity. According to the k_T factorization, the momenta k_1, k_2 in the M^+ meson and k_3, k_4 in the M^- meson as labeled in Fig. 1 can be written as

$$\begin{aligned} k_1 &= (2x\omega, 0, \mathbf{k}_{\perp 1}), & k_2 &= (2\bar{x}\omega, 0, -\mathbf{k}_{\perp 1}), \\ k_3 &= (2y\omega, 0, \mathbf{k}_{\perp 2}), & k_4 &= (2\bar{y}\omega, 0, -\mathbf{k}_{\perp 2}), \end{aligned} \quad (2)$$

with $\bar{x} \equiv 1 - x$ ($\bar{y} \equiv 1 - y$), x and \bar{x} are the longitudinal momentum fractions of quark and antiquark, respectively. The intrinsic transverse momenta $\mathbf{k}_{\perp 1}, \mathbf{k}_{\perp 2}$ are relate to the momenta of the two out-going mesons. The polarization states of the photons are taken to be

$$\begin{aligned} \varepsilon_1^+ &= \frac{1}{\sqrt{2}}(2sc, -2sc, s^2 - c^2, -i), & \varepsilon_1^- &= \frac{1}{\sqrt{2}}(-2sc, 2sc, c^2 - s^2, -i), \\ \varepsilon_2^+ &= \frac{1}{\sqrt{2}}(-2sc, 2sc, c^2 - s^2, -i), & \varepsilon_2^- &= \frac{1}{\sqrt{2}}(2sc, -2sc, s^2 - c^2, -i). \end{aligned} \quad (3)$$

B. Light-cone wave functions

The Fierz identity is generally employed to factorize the fermion flow:

$$\begin{aligned} \bar{q}_{1\alpha} q_{2\beta} &= \frac{1}{4} I_{\beta\alpha} (\bar{q}_1 q_2) - \frac{1}{4} (i\gamma_5)_{\beta\alpha} (\bar{q}_1 i\gamma_5 q_2) + \frac{1}{4} (\gamma_\mu)_{\beta\alpha} (\bar{q}_1 \gamma^\mu q_2) \\ &\quad - \frac{1}{4} (\gamma_\mu \gamma_5)_{\beta\alpha} (\bar{q}_1 \gamma^\mu \gamma_5 q_2) + \frac{1}{8} (\sigma_{\mu\nu} \gamma_5)_{\beta\alpha} (\bar{q}_1 \sigma^{\mu\nu} \gamma_5 q_2). \end{aligned} \quad (4)$$

Here q and \bar{q} are the quark and antiquark field. The Dirac structure $\gamma^\mu \gamma^5$ in Eq. (4) contributes at the twist-2 level, while $i\gamma^5$ and $\sigma^{\mu\nu} \gamma^5$ contribute at the twist-3 level.

Following the definition of distribution amplitudes with leading and next-to-leading twist [41, 42], the light-cone wave functions of pion can be expressed via the matrix element of the bilocal operator

$$\begin{aligned} \langle \pi(p) | \bar{q}_\beta(z_1) q_\alpha(z_2) | 0 \rangle &= \frac{if_\pi}{4} \int_0^1 dx \int \frac{d^2 \mathbf{k}_\perp}{16\pi^3} e^{i(xp \cdot z_1 + \bar{x}p \cdot z_2 - \mathbf{k}_\perp \cdot (\mathbf{z}_{1\perp} - \mathbf{z}_{2\perp}))} \\ &\quad \times \left\{ \not{p} \gamma_5 \Psi_\pi(x, \mathbf{k}_\perp) - \mu_\pi \gamma_5 \left(\Psi_p(x, \mathbf{k}_\perp) - \sigma_{\mu\nu} p^\mu (z_1 - z_2)^\nu \frac{\Psi_\sigma(x, \mathbf{k}_\perp)}{6} \right) \right\}_{\alpha\beta}, \end{aligned} \quad (5)$$

where f_π refers to the decay constant of pion and the mass parameter μ_π defined as

$$\mu_\pi = \frac{m_\pi^2}{m_u + m_d}, \quad (6)$$

which can be related to the chiral condensate. Here m_u, m_d are the current quark masses and m_π denotes the pion meson mass. Ψ_π is the twist-2 wave function and Ψ_p, Ψ_σ are two two-particle twist-3 wave functions. Generally, the twist-3 contributions are power suppressed. However, at the intermediate energy region (such as the BELLE experimental range), the suppression factor $\frac{\mu_\pi^2}{Q^2} \sim \mathcal{O}(1)$ in the twist-3 contributions is not small enough, so the twist-3 contributions should be taken into consideration.

By transforming the Eq. (5) from the coordinate space into the momentum space, one can obtain the light-cone projection operator [37, 43, 44]

$$M_{\alpha\beta}^\pi = \frac{if_\pi}{4} \left\{ \not{p} \gamma_5 \Psi_\pi - \mu_\pi \gamma_5 \left(\Psi_p - i\sigma_{\mu\nu} \frac{p^\mu \bar{p}^\nu}{p \cdot \bar{p}} \frac{\Psi'_\sigma}{6} + i\sigma_{\mu\nu} p^\mu \frac{\Psi_\sigma}{6} \frac{\partial}{\partial k_{\perp\nu}} \right) \right\}_{\alpha\beta} \quad (7)$$

with $\Psi'_\sigma = \frac{\partial \Psi_\sigma(x, \mathbf{k}_\perp)}{\partial x}$. The dependence of the transverse momentum may be different in the wave functions Ψ_π, Ψ_p and Ψ_σ , which makes the numerical calculation more complicated. For the convenience of calculations, we assume that these wave functions have the same transverse momentum dependence.

The intrinsic transverse momentum dependence of wave function of pion is still unknown from the first principle in QCD. Following the ansatz made in Refs. [32, 45], the longitudinal and transverse momentum dependence of the wave function can be separated into two parts

$$\Psi(x, \mathbf{k}_\perp, \mu) = \phi(x, \mu)\Sigma(x, \mathbf{k}_\perp), \quad (8)$$

where $\phi(x, \mu)$ is the pion distribution amplitude. The functions $\phi(x, \mu)$ and $\Sigma(x, \mathbf{k}_\perp)$ satisfy the normalization conditions

$$\int_0^1 dx \phi(x, \mu) = 1, \quad \int \frac{d^2\mathbf{k}_\perp}{16\pi^3} \Sigma(x, \mathbf{k}_\perp) = 1. \quad (9)$$

The particular k_\perp -dependence of wave function is contained in the function $\Sigma(x, k_\perp)$ and it is usually assumed to be a simple Gaussian form [32]

$$\Sigma(x, \mathbf{k}_\perp) = \frac{16\pi^2\beta^2}{x(1-x)} \exp\left[-\frac{\beta^2\mathbf{k}_\perp^2}{x(1-x)}\right]. \quad (10)$$

In perturbative QCD approach, the convolution of wave functions and hard scattering kernels is conventionally presented in the transverse configuration b -space. So we need the Fourier transform of the k_\perp -dependence part of the wave function

$$\hat{\Sigma}(x, b) = 4\pi \exp\left[-\frac{x(1-x)b^2}{4\beta^2}\right]. \quad (11)$$

The impact parameter b represents the transverse separation between the quark and antiquark in pion. Then the full soft wave function of pion in the transverse configuration b -space reads

$$\hat{\Psi}(x, b, \mu) = \phi(x, \mu)\hat{\Sigma}(x, b). \quad (12)$$

The oscillator parameter β in the above equations is determined by the root mean square transverse momentum

$$\langle \mathbf{k}_\perp^2 \rangle = \frac{\int_0^1 dx \int d^2\mathbf{k}_\perp \mathbf{k}_\perp^2 |\Psi(x, \mathbf{k}_\perp)|^2}{\int_0^1 dx \int d^2\mathbf{k}_\perp |\Psi(x, \mathbf{k}_\perp)|^2} = \frac{1}{2\beta^2} \frac{\int_0^1 dx |\phi(x)|^2}{\int_0^1 dx \frac{|\phi(x)|^2}{x(1-x)}}. \quad (13)$$

The detailed discussions about the choice of the oscillator parameter β are shown in Ref. [32]. In this work, we will take the value $\langle \mathbf{k}_\perp^2 \rangle_{\pi, K}^{1/2} = 0.35$ GeV.

The longitudinal dependence of the leading-twist wave functions, i.e. the twist-2 distribution amplitudes, for pion and kaon meson with the expansion of Gegenbauer polynomials at a scale μ read [46, 47]

$$\phi_\pi(x, \mu) = 6x(1-x)[1 + a_2^\pi(\mu^2)C_2^{3/2}(2x-1) + a_4^\pi(\mu^2)C_4^{3/2}(2x-1)], \quad (14)$$

$$\phi_K(x, \mu) = 6x(1-x)[1 + a_1^K(\mu^2)C_1^{3/2}(2x-1) + a_2^K(\mu^2)C_2^{3/2}(2x-1)]. \quad (15)$$

To leading logarithmic accuracy, the nonperturbative Gegenbauer moments a_n^i are renormalized multiplicatively with

$$a_n^i(\mu^2) = L^{4\gamma_n/\beta_1} a_n^i(\mu_0^2), \quad (16)$$

with $L \equiv \alpha_s(\mu^2)/\alpha_s(\mu_0^2)$, $\beta_1 = (11N_c - 2N_f)/12$. We take $n = 2, 4$ in the pion distribution amplitude (Eq. (14)) for SU(2) isotopic symmetry and $n = 1, 2$ in the kaon distribution amplitude (Eq. (15)) for SU(3)-flavor symmetry breaking. The anomalous dimension γ_n is given by

$$\gamma_n = 4C_F \left(\psi(n+2) + \gamma_E - \frac{3}{4} - \frac{1}{2(n+1)(n+2)} \right). \quad (17)$$

We prefer to choose the Gegenbauer moments a_n^i at $\mu_0 = 1$ GeV as follows, quoted from Ref. [48]

$$\begin{aligned} a_2^\pi(1 \text{ GeV}) &= 0.115, & a_4^\pi(1 \text{ GeV}) &= -0.015, \\ a_1^K(1 \text{ GeV}) &= 0.170, & a_2^K(1 \text{ GeV}) &= 0.115. \end{aligned} \quad (18)$$

Those coefficients a_n^i of Gegenbauer polynomials are in agreement with the recent lattice QCD results [49–51].

As for the twist-3 distribution amplitudes of pion and kaon, we take the asymptotic forms for simplicity, i.e.

$$\phi_p^{asy}(x) = 1, \quad \phi_\sigma^{asy}(x) = 6x(1-x). \quad (19)$$

C. The twist-3 contributions and the modified perturbative QCD approach

The differential cross section of the collision process $\gamma\gamma \rightarrow \pi^+\pi^-$ can be expressed as

$$\frac{d\sigma(\gamma\gamma \rightarrow \pi^+\pi^-)}{d|\cos\theta|} = \frac{1}{32\pi Q^2} \frac{1}{4} \sum_{\lambda_1, \lambda_2 = \pm 1} |\mathcal{M}_{\lambda_1\lambda_2}|^2. \quad (20)$$

In the modified QCD perturbative approach, the helicity amplitude $\mathcal{M}_{\lambda_1\lambda_2}$ can be written as the convolution of the universal hadron wave functions and the hard scattering kernels by both longitudinal momentum fractions x, y and transverse separation scales $\mathbf{b}_1, \mathbf{b}_2$ of the pions [52]

$$\begin{aligned} \mathcal{M}_{\lambda_1\lambda_2}(Q, \theta) = & \int_0^1 dx dy \int \frac{d^2\mathbf{b}_1}{4\pi} \frac{d^2\mathbf{b}_2}{4\pi} \sum_{i,j=\pi,p,\sigma,\sigma'} \hat{\Psi}_i(x, \mathbf{b}_1, \mu_F) \hat{T}_{ij}^{\lambda_1\lambda_2}(x, y, Q, \theta, \mathbf{b}_1, \mathbf{b}_2, \mu_R) \hat{\Psi}_j(y, \mathbf{b}_2, \mu_F) \\ & \times S_t(x) S_t(y) \exp[-S(x, y, \mathbf{b}_1, \mathbf{b}_2, \mu_F, \mu_R)], \end{aligned} \quad (21)$$

with

$$\hat{\Psi}_{\sigma'}(x, \mathbf{b}_1, \mu_F) = \frac{\partial \hat{\Psi}_\sigma(x, \mathbf{b}_1, \mu_F)}{\partial x}, \quad \hat{\Psi}_{\sigma'}(y, \mathbf{b}_2, \mu_F) = \frac{\partial \hat{\Psi}_\sigma(y, \mathbf{b}_2, \mu_F)}{\partial y}. \quad (22)$$

Here the scripts $i, j = \pi$ correspond to twist-2 wave function and $i, j = p, \sigma, \sigma'$ correspond to twist-3 wave functions. $\hat{T}_{ij}^{\lambda_1\lambda_2}$ is the Fourier transform of the hard scattering amplitude $T_{ij}^{\lambda_1\lambda_2}$ with the intrinsic transverse momentum dependence retained

$$\begin{aligned} \hat{T}_{ij}^{\lambda_1\lambda_2}(x, y, Q, \theta, \mathbf{b}_1, \mathbf{b}_2, \mu_R) = & \int \frac{d^2\mathbf{k}_{\perp 1}}{(2\pi)^2} \frac{d^2\mathbf{k}_{\perp 2}}{(2\pi)^2} T_{ij}^{\lambda_1\lambda_2}(x, y, Q, \theta, \mathbf{k}_{\perp 1}, \mathbf{k}_{\perp 2}, \mu_R) \\ & \times \exp[-i\mathbf{k}_{\perp 1} \cdot \mathbf{b}_1 - i\mathbf{k}_{\perp 2} \cdot \mathbf{b}_2]. \end{aligned} \quad (23)$$

$T_{ij}^{\lambda_1\lambda_2}$ can be calculated from the Feynman diagrams and the nonzero terms for the hard scattering amplitudes with the scripts $ij = \pi\pi, pp, p\sigma(p\sigma'), \sigma p(\sigma'p), \sigma\sigma(\sigma'\sigma, \sigma\sigma', \sigma'\sigma')$ including the twist-3 contributions.

In the following calculation, we will show our procedure to the Fourier transform of the hard scattering kernels by means of a specific Feynman diagram in the Group **a** in Fig. 1 as an example. The hard kernels $T_{a_1 ij}^{\lambda_1\lambda_2}$ with the subscript “ a_1 ” specifically refer to the results of one of the six diagrams in Group **a**. Its leading twist contributions are illustrated as

$$\begin{aligned} T_{a_1 \pi\pi}^{++}(x, y, Q, \theta, \mathbf{k}_{\perp 1}, \mathbf{k}_{\perp 2}, \mu_R) &= \frac{1024}{81} \frac{i\kappa_1 s^2 c^2 \omega^4 (xy + \bar{x}\bar{y})}{(\tilde{q}_1^2 + i\epsilon)(\tilde{q}_2^2 + i\epsilon)(\tilde{g}^2 + i\epsilon)}, \\ T_{a_1 \pi\pi}^{+-}(x, y, Q, \theta, \mathbf{k}_{\perp 1}, \mathbf{k}_{\perp 2}, \mu_R) &= \frac{1024}{81} \frac{i\kappa_1 s^2 c^2 \omega^4 (\bar{x}y + x\bar{y})}{(\tilde{q}_1^2 + i\epsilon)(\tilde{q}_2^2 + i\epsilon)(\tilde{g}^2 + i\epsilon)}, \end{aligned} \quad (24)$$

with the factor $\kappa_1 = \alpha\alpha_s(\mu_R)\pi^2 f_\pi^2$. The corresponding quark and gluon propagators are

$$\begin{aligned} \tilde{q}_1^2 &= 4s^2(x - s^2)\omega^2 - (\mathbf{p} - \mathbf{k}_{\perp 1})^2, \\ \tilde{q}_2^2 &= 4s^2(\bar{y} - s^2)\omega^2 - (\mathbf{p} + \mathbf{k}_{\perp 2})^2, \\ \tilde{g}^2 &= 4\bar{x}y\omega^2 - \mathbf{K}_\perp^2, \end{aligned} \quad (25)$$

with

$$\mathbf{K}_\perp = \mathbf{k}_{\perp 1} - \mathbf{k}_{\perp 2}. \quad (26)$$

The convolution formula Eq. (21) involves two independent scales of this process, the factorization scale μ_F and the renormalization scale μ_R . In analogy to the cases of the pion's electromagnetic form factor [30, 31] and transition form factor [53], the transverse separation scales b_1 and b_2 of the pion wave functions provide the factorization scales $\mu_{Fi} = 1/b_i$ ($i = 1, 2$) and the renormalization scale $\mu_R = t$ corresponding to the maximum of the longitudinal and transverse scales associated with the hard gluon.

In the hard scattering kernels, the terms contained the transverse momentum \mathbf{k}_\perp in the numerators are power suppressed and they must be dropped in order to ensure the gauge invariance required by the factorization theorem. Since the k_T factorization theorem applies to processes dominated by small x contribution, the hierarchy $s^2 x \omega^2, s^2 \bar{y} \omega^2 \gg \bar{x} y \omega^2, \mathbf{k}_\perp^2$ can be adopted. Only

the transverse momentum \mathbf{k}_\perp in the gluon propagator is retained to regulate the endpoint singularity, see Refs. [34, 37, 38, 54] for more detailed discussion. Then the forms of Eq. (24) are reduced to

$$\begin{aligned} T_{a_1\pi\pi}^{++}(x, y, Q, \theta, \mathbf{k}_{\perp 1}, \mathbf{k}_{\perp 2}, \mu_R) &= \frac{64}{81} \frac{\nu\kappa_1 c^2 (xy + \bar{x}\bar{y})}{s^2 x\bar{y}} \frac{1}{(\tilde{g}^2 + \nu\epsilon)}, \\ T_{a_1\pi\pi}^{+-}(x, y, Q, \theta, \mathbf{k}_{\perp 1}, \mathbf{k}_{\perp 2}, \mu_R) &= \frac{64}{81} \frac{\nu\kappa_1 c^2 (\bar{x}y + x\bar{y})}{s^2 x\bar{y}} \frac{1}{(\tilde{g}^2 + \nu\epsilon)}. \end{aligned} \quad (27)$$

Since the $T_{a_1 i j}^{\lambda_1 \lambda_2}$ depends on $\mathbf{k}_{\perp 1}$ and $\mathbf{k}_{\perp 2}$ only in the combination \mathbf{K}_\perp , the expression for the Fourier transform of the hard scattering amplitude now involves only a single \mathbf{b} ($=|\mathbf{b}|$) parameter

$$\begin{aligned} \hat{T}_{a_1\pi\pi}^{++}(x, y, Q, \theta, \mathbf{b}, \mu_R) &= \frac{16\kappa_1}{81} \frac{c^2 (xy + \bar{x}\bar{y})}{s^2 x\bar{y}} H_0^{(1)}(2\omega\sqrt{\bar{x}y}b), \\ \hat{T}_{a_1\pi\pi}^{+-}(x, y, Q, \theta, \mathbf{b}, \mu_R) &= \frac{16\kappa_1}{81} \frac{c^2 (\bar{x}y + x\bar{y})}{s^2 x\bar{y}} H_0^{(1)}(2\omega\sqrt{\bar{x}y}b). \end{aligned} \quad (28)$$

Here $H_0^{(1)}$ and K_0 denote Hankel and modified Bessel function, which come from the Fourier transform of the gluon propagators regularizable with the $\nu\epsilon$ prescription

$$\int \frac{d^2\mathbf{k}_\perp}{(2\pi)^2} \frac{\exp[-i\mathbf{k}_\perp \cdot \mathbf{b}]}{s - \mathbf{k}_\perp^2 + \nu\epsilon} = \begin{cases} -\frac{i}{4} H_0^{(1)}(\sqrt{s}b) & \text{for } s > 0 \\ -\frac{1}{2\pi} K_0(\sqrt{-s}b) & \text{for } s < 0 \end{cases}. \quad (29)$$

The single b dependence enormously simplifies the numerical calculation, which means the two pions emerge from collision with the identical transverse separations in this approximation.

The unique part of the modified perturbative QCD approach is the Sudakov factor $\exp[-S]$, which comprises the double logarithms produced by overlapping collinear and soft divergencies for massless quarks and absorbs the renormalization group factor from the hadronic wave functions and hard scattering amplitude. The expression for the Sudakov exponent in next-to-leading logarithm approximation is given by [30]

$$S(x, y, b, Q, t) = s(x, b, Q) + s(\bar{x}, b, Q) + s(y, b, Q) + s(\bar{y}, b, Q) - \frac{2}{\beta_1} \ln \frac{\ln(t/\Lambda_{QCD})}{\ln(1/(b/\Lambda_{QCD}))}, \quad (30)$$

where the function $s(x, b, Q)$, originally derived by Botts and Sterman [29] and later on slightly improved, for instance, in Refs. [30, 55]. The explicit expression of $s(x, b, Q)$ is given in Appendix. The last term in Eq. (30) arises from a renormalization group transformation from the factorization scale $1/b$ to the renormalization scale t at which the hard amplitude \hat{T}_H is evaluated. The renormalization scale t is the largest mass scale appearing in T_H which associates with the momentum of the internal hard gluon propagators in the collinear limit and $1/b$ related to the transverse momentum of quarks in the meson. This selection method avoids the large logarithms from higher-order perturbative QCD corrections effectively. The Sudakov factor $\exp[-S]$, exhibiting a strong fall off at large b , vanishes for $b > 1/\Lambda_{QCD}$ to ensure the contributions dominated by the hard scattering.

As for the twist-3 case, the Sudakov factor $\exp[-S]$ still may not be effective enough to suppress the nonperturbative contributions due to the end-point singularities. As pointed out in Refs. [37, 38, 56–59], when the endpoint contribution is important, the threshold resummation effects, which organize the large double logarithms $\ln^2 x$ into a jet function $S_t(x)$, should be taken into account. This double logarithms, as analyzed in Ref. [56], appearing in the QCD loop corrections for the electromagnetic vertex should be organized to all orders in order to improve perturbative expansion. The jet function vanishes as $x \rightarrow 0, 1$, and modifies the end-point behavior of meson distribution amplitudes effectively. We employ the parametrization form proposed in Refs. [38, 56]

$$S_t(x, Q) = \frac{2^{1+2c}\Gamma(3/2+c)}{\sqrt{\pi}\Gamma(1+c)} [x(1-x)]^c, \quad (31)$$

In Ref. [57], Li and Mishima have proposed a parabolic parametrization for the parameter c , and freeze c at $c = 1$, when it exceeds unity:

$$c(Q^2) = 0.04Q^2 - 0.51Q + 1.87. \quad (32)$$

The factor $S_t(x)$ further suppresses the end-point behaviors of the pion distribution amplitudes, especially for the twist-3 ones, and makes perturbative QCD approach more applicable.

Taking all of the above mentioned effects into account, one can rewrite the helicity amplitude of Eq.(21) to a much clearer and simpler form in the conjugate b space

$$\begin{aligned} \mathcal{M}_{\lambda_1\lambda_2}(Q, \theta) &= \int_0^1 dx dy \int \frac{d^2\mathbf{b}}{(4\pi)^2} \sum_{i,j=\pi,p,\sigma,\sigma'} \hat{\Psi}_i(x, \mathbf{b}, \frac{1}{b}) \hat{T}_{\lambda_1\lambda_2}^{ij}(x, y, Q, \theta, \mathbf{b}, t) \hat{\Psi}_j(y, \mathbf{b}, \frac{1}{b}) \\ &\times S_t(x) S_t(y) \exp[-S(x, y, Q, b, t)]. \end{aligned} \quad (33)$$

Making the substitution $\int d^2\mathbf{b} \rightarrow \int b db d\varphi$ and performing the integral over the polar angle φ , we can obtain the helicity amplitudes for $\gamma\gamma \rightarrow \pi^+\pi^-$ process in the conjugate b space by summing up all the twenty Feynman diagrams in four types

$$\begin{aligned} \mathcal{M}_{\lambda_1\lambda_2}(Q, \theta) &= \int_0^1 dx dy \int \frac{bdb}{(4\pi)^2} \sum_{n=a}^{b,c,d} \left(\sum_{i,j=\pi}^{p,\sigma,\sigma'} \hat{\Psi}_i(x, b, \frac{1}{b}) \hat{T}_{nij}^{\lambda_1\lambda_2}(x, y, Q, \theta, b, t_n) \hat{\Psi}_j(y, b, \frac{1}{b}) \right. \\ &\left. \times S_t(x) S_t(y) \exp[-S(x, y, Q, b, t_n)] \right), \end{aligned} \quad (34)$$

with the twist-2 hard kernels

$$\begin{aligned} \hat{T}_{a\pi\pi}^{+++} &= \frac{16\kappa_1}{81} \frac{xy + \bar{x}\bar{y}}{s^2 c^2 x\bar{y}} F(s_a, b), \\ \hat{T}_{b\pi\pi}^{+++} &= \frac{4\kappa_1}{81} \frac{xy + \bar{x}\bar{y}}{s^2 c^2 \bar{x}y} F(s_b, b), \\ \hat{T}_{c\pi\pi}^{+++} &= -\frac{8\kappa_1}{81} \left(\frac{xy + \bar{x}\bar{y}}{s^2 c^2 xy} + \frac{(xy + \bar{x}\bar{y})(x - \bar{y})}{c^2 x\bar{y}\bar{y}} \right) J_0(-pb) F(s_c, b), \\ \hat{T}_{d\pi\pi}^{+++} &= -\frac{8\kappa_1}{81} \left(\frac{xy + \bar{x}\bar{y}}{s^2 c^2 \bar{x}\bar{y}} + \frac{(xy + \bar{x}\bar{y})(\bar{x} - y)}{c^2 x\bar{y}y} \right) J_0(pb) F(s_d, b), \end{aligned} \quad (35)$$

$$\begin{aligned} \hat{T}_{a\pi\pi}^{+-} &= \frac{16\kappa_1}{81} \left(4 + \frac{s^2(\bar{x}y + x\bar{y})}{c^2 x\bar{y}} + \frac{c^2(\bar{x}y + x\bar{y})}{s^2 x\bar{y}} \right) F(s_a, b), \\ \hat{T}_{b\pi\pi}^{+-} &= \frac{4\kappa_1}{81} \left(4 + \frac{s^2(\bar{x}y + x\bar{y})}{c^2 \bar{x}y} + \frac{c^2(\bar{x}y + x\bar{y})}{s^2 \bar{x}y} \right) F(s_b, b), \\ \hat{T}_{c\pi\pi}^{+-} &= \frac{8\kappa_1}{81} \left(4 - \frac{s^2(\bar{x}y + x\bar{y})}{c^2 \bar{x}\bar{y}} - \frac{c^2(\bar{x}y + x\bar{y})}{s^2 xy} \right) J_0(-pb) F(s_c, b), \\ \hat{T}_{d\pi\pi}^{+-} &= \frac{8\kappa_1}{81} \left(4 - \frac{s^2(\bar{x}y + x\bar{y})}{c^2 xy} - \frac{c^2(\bar{x}y + x\bar{y})}{s^2 \bar{x}\bar{y}} \right) J_0(pb) F(s_d, b), \end{aligned} \quad (36)$$

and the nonzero twist-3 hard kernels

$$\begin{aligned} \hat{T}_{app}^{+++} &= -\frac{8\kappa_2}{81} \left(2 - \frac{1 - \bar{x}y}{s^2 x\bar{y}} - \frac{1 - \bar{x}y}{c^2 x\bar{y}} \right) F(s_a, b), & \hat{T}_{app}^{+-} &= \frac{8\kappa_2}{81} \left(\frac{1}{s^2 c^2} - \frac{2(1 - x\bar{y})}{\bar{x}y} \right) F(s_a, b), \\ \hat{T}_{bpp}^{+++} &= -\frac{2\kappa_2}{81} \left(2 - \frac{1 - x\bar{y}}{s^2 \bar{x}y} - \frac{1 - x\bar{y}}{c^2 \bar{x}y} \right) F(s_b, b), & \hat{T}_{bpp}^{+-} &= \frac{2\kappa_2}{81} \left(\frac{1}{s^2 c^2} - \frac{2(1 - \bar{x}y)}{x\bar{y}} \right) F(s_b, b), \\ \hat{T}_{cpp}^{+++} &= \frac{4\kappa_2}{81} \left(2 + \frac{1 - \bar{x}\bar{y}}{s^2 xy} + \frac{1 - xy}{c^2 \bar{x}\bar{y}} \right) J_0(-pb) F(s_c, b), & \hat{T}_{cpp}^{+-} &= \frac{4\kappa_2}{81} \left(\frac{1}{s^2 c^2} - 2 \right) J_0(-pb) F(s_c, b), \\ \hat{T}_{dpp}^{+++} &= \frac{4\kappa_2}{81} \left(2 + \frac{1 - xy}{s^2 \bar{x}\bar{y}} + \frac{1 - \bar{x}\bar{y}}{c^2 xy} \right) J_0(pb) F(s_d, b), & \hat{T}_{dpp}^{+-} &= \frac{4\kappa_2}{81} \left(\frac{1}{s^2 c^2} - 2 \right) J_0(pb) F(s_d, b), \end{aligned} \quad (37)$$

$$\begin{aligned} \hat{T}_{cp\sigma}^{+++} &= -\frac{2\kappa_2}{243} \frac{\omega b (s^2 x + c^2 \bar{x})}{scx\bar{x}} J_1(-pb) F(s_c, b), & \hat{T}_{cp\sigma}^{+-} &= -\frac{2\kappa_2}{243} \frac{\omega b (s^2 \bar{x} + c^2 x + 1)}{scx\bar{x}} J_1(-pb) F(s_c, b), \\ \hat{T}_{dp\sigma}^{+++} &= \frac{2\kappa_2}{243} \frac{\omega b (s^2 \bar{x} + c^2 x)}{scx\bar{x}} J_1(pb) F(s_d, b), & \hat{T}_{dp\sigma}^{+-} &= \frac{2\kappa_2}{243} \frac{\omega b (s^2 x + c^2 \bar{x} + 1)}{scx\bar{x}} J_1(pb) F(s_d, b), \end{aligned} \quad (38)$$

$$\begin{aligned}
\hat{T}_{ap\sigma'}^{+++} &= \frac{4\kappa_2}{243} \left(\frac{1}{s^2c^2} - \frac{2}{x} \right) F(s_a, b), & \hat{T}_{ap\sigma'}^{+--} &= \frac{4\kappa_2}{243} \left(\frac{\bar{x}^2}{s^2c^2x\bar{x}} - \frac{2}{x\bar{x}} \right) F(s_a, b), \\
\hat{T}_{bp\sigma'}^{+++} &= -\frac{\kappa_2}{243} \left(\frac{1}{s^2c^2} - \frac{2}{\bar{x}} \right) F(s_b, b), & \hat{T}_{bp\sigma'}^{+--} &= -\frac{\kappa_2}{243} \left(\frac{x^2}{s^2c^2x\bar{x}} - \frac{2}{x\bar{x}} \right) F(s_b, b), \\
\hat{T}_{cp\sigma'}^{+++} &= -\frac{2\kappa_2}{243} \left(\frac{s^2 - c^2}{s^2c^2} - \frac{x - \bar{x}}{x\bar{x}} \right) J_0(-pb)F(s_c, b), & \hat{T}_{cp\sigma'}^{+--} &= -\frac{2\kappa_2}{243} \left(\frac{s^2x^2 - c^2\bar{x}^2}{s^2c^2x\bar{x}} + \frac{x - \bar{x}}{x\bar{x}} \right) J_0(-pb)F(s_c, b), \\
\hat{T}_{dp\sigma'}^{+++} &= -\frac{2\kappa_2}{243} \left(\frac{c^2 - s^2}{s^2c^2} - \frac{x - \bar{x}}{x\bar{x}} \right) J_0(pb)F(s_d, b), & \hat{T}_{dp\sigma'}^{+--} &= -\frac{2\kappa_2}{243} \left(\frac{c^2x^2 - s^2\bar{x}^2}{s^2c^2x\bar{x}} + \frac{x - \bar{x}}{x\bar{x}} \right) J_0(pb)F(s_d, b), \quad (39)
\end{aligned}$$

$$\begin{aligned}
\hat{T}_{c\sigma p}^{+++} &= \frac{2\kappa_2}{243} \frac{\omega b (s^2y + c^2\bar{y})}{scy\bar{y}} J_1(-pb)F(s_c, b), & \hat{T}_{c\sigma p}^{+--} &= \frac{2\kappa_2}{243} \frac{\omega b (s^2\bar{y} + c^2y + 1)}{scy\bar{y}} J_1(-pb)F(s_c, b), \\
\hat{T}_{d\sigma p}^{+++} &= -\frac{2\kappa_2}{243} \frac{\omega b (s^2\bar{y} + c^2y)}{scy\bar{y}} J_1(pb)F(s_d, b), & \hat{T}_{d\sigma p}^{+--} &= -\frac{2\kappa_2}{243} \frac{\omega b (s^2y + c^2\bar{y} + 1)}{scy\bar{y}} J_1(pb)F(s_d, b), \quad (40)
\end{aligned}$$

$$\begin{aligned}
\hat{T}_{a\sigma'p}^{+++} &= \frac{4\kappa_2}{243} \left(\frac{1}{s^2c^2} - \frac{2}{\bar{y}} \right) F(s_a, b), & \hat{T}_{a\sigma'p}^{+--} &= \frac{4\kappa_2}{243} \left(\frac{y^2}{s^2c^2y\bar{y}} - \frac{2}{y\bar{y}} \right) F(s_a, b), \\
\hat{T}_{b\sigma'p}^{+++} &= -\frac{\kappa_2}{243} \left(\frac{1}{s^2c^2} - \frac{2}{y} \right) F(s_b, b), & \hat{T}_{b\sigma'p}^{+--} &= -\frac{\kappa_2}{243} \left(\frac{\bar{y}^2}{s^2c^2y\bar{y}} - \frac{2}{y\bar{y}} \right) F(s_b, b), \\
\hat{T}_{c\sigma'p}^{+++} &= \frac{2\kappa_2}{243} \left(\frac{s^2 - c^2}{s^2c^2} - \frac{y - \bar{y}}{y\bar{y}} \right) J_0(-pb)F(s_c, b), & \hat{T}_{c\sigma'p}^{+--} &= \frac{2\kappa_2}{243} \left(\frac{s^2y^2 - c^2\bar{y}^2}{s^2c^2y\bar{y}} + \frac{y - \bar{y}}{y\bar{y}} \right) J_0(-pb)F(s_c, b), \\
\hat{T}_{d\sigma'p}^{+++} &= \frac{2\kappa_2}{243} \left(\frac{c^2 - s^2}{s^2c^2} - \frac{y - \bar{y}}{y\bar{y}} \right) J_0(pb)F(s_d, b), & \hat{T}_{d\sigma'p}^{+--} &= \frac{2\kappa_2}{243} \left(\frac{c^2y^2 - s^2\bar{y}^2}{s^2c^2y\bar{y}} + \frac{y - \bar{y}}{y\bar{y}} \right) J_0(pb)F(s_d, b), \quad (41)
\end{aligned}$$

$$\begin{aligned}
\hat{T}_{c\sigma\sigma}^{+--} &= -\frac{2\kappa_2}{729} \left(\frac{\omega^2b^2}{xy} + \frac{\omega^2b^2}{\bar{x}\bar{y}} \right) J_2(-pb)F(s_c, b), \\
\hat{T}_{d\sigma\sigma}^{+--} &= -\frac{2\kappa_2}{729} \left(\frac{\omega^2b^2}{xy} + \frac{\omega^2b^2}{\bar{x}\bar{y}} \right) J_2(pb)F(s_d, b), \quad (42)
\end{aligned}$$

$$\begin{aligned}
\hat{T}_{c\sigma\sigma'}^{+++} &= \frac{\kappa_2}{729} \left(\frac{\omega bc}{sy} - \frac{\omega bs}{c\bar{y}} \right) J_1(-pb)F(s_c, b), & \hat{T}_{c\sigma\sigma'}^{+--} &= \frac{\kappa_2}{729} \left(\frac{\omega bc(1 + \bar{x})}{sxy} - \frac{\omega bs(1 + x)}{c\bar{x}\bar{y}} \right) J_1(-pb)F(s_c, b), \\
\hat{T}_{d\sigma\sigma'}^{+++} &= \frac{\kappa_2}{729} \left(\frac{\omega bc}{s\bar{y}} - \frac{\omega bs}{cy} \right) J_1(pb)F(s_d, b), & \hat{T}_{d\sigma\sigma'}^{+--} &= \frac{\kappa_2}{729} \left(\frac{\omega bc(1 + x)}{s\bar{x}\bar{y}} - \frac{\omega bs(1 + \bar{x})}{cxy} \right) J_1(pb)F(s_d, b), \quad (43)
\end{aligned}$$

$$\begin{aligned}
\hat{T}_{c\sigma'\sigma}^{+++} &= \frac{\kappa_2}{729} \left(\frac{\omega bc}{sx} - \frac{\omega bs}{c\bar{x}} \right) J_1(-pb)F(s_c, b), & \hat{T}_{c\sigma'\sigma}^{+--} &= \frac{\kappa_2}{729} \left(\frac{\omega bc(1 + \bar{y})}{sxy} - \frac{\omega bs(1 + y)}{c\bar{x}\bar{y}} \right) J_1(-pb)F(s_c, b), \\
\hat{T}_{d\sigma'\sigma}^{+++} &= \frac{\kappa_2}{729} \left(\frac{\omega bc}{s\bar{x}} - \frac{\omega bs}{cx} \right) J_1(pb)F(s_d, b), & \hat{T}_{d\sigma'\sigma}^{+--} &= \frac{\kappa_2}{729} \left(\frac{\omega bc(1 + y)}{s\bar{x}\bar{y}} - \frac{\omega bs(1 + \bar{y})}{cxy} \right) J_1(pb)F(s_d, b), \quad (44)
\end{aligned}$$

$$\begin{aligned}
\hat{T}_{a\sigma'\sigma'}^{+++} &= \frac{2\kappa_2}{729} \left(\frac{s^2(1 - \bar{x}y)}{c^2x\bar{y}} + \frac{c^2(1 - \bar{x}y)}{s^2x\bar{y}} \right) F(s_a, b), \\
\hat{T}_{b\sigma'\sigma'}^{+++} &= \frac{\kappa_2}{1458} \left(\frac{s^2(1 - x\bar{y})}{c^2\bar{x}y} + \frac{c^2(1 - x\bar{y})}{s^2\bar{x}y} \right) F(s_b, b), \\
\hat{T}_{c\sigma'\sigma'}^{+++} &= -\frac{\kappa_2}{729} \left(\frac{s^2(1 - xy)}{c^2\bar{x}\bar{y}} + \frac{c^2(1 - \bar{x}y)}{s^2xy} \right) J_0(-pb)F(s_c, b), \\
\hat{T}_{d\sigma'\sigma'}^{+++} &= -\frac{\kappa_2}{729} \left(\frac{s^2(1 - \bar{x}\bar{y})}{c^2xy} + \frac{c^2(1 - xy)}{s^2\bar{x}\bar{y}} \right) J_0(pb)F(s_d, b), \quad (45)
\end{aligned}$$

$$\begin{aligned}
\hat{T}_{a\sigma'\sigma'}^{+-} &= \frac{2\kappa_2}{729} \left(\frac{s^2(1+\bar{x}y)}{c^2\bar{x}\bar{y}} + \frac{c^2(1+\bar{x}y)}{s^2\bar{x}\bar{y}} \right) F(s_a, b), \\
\hat{T}_{b\sigma'\sigma'}^{+-} &= \frac{\kappa_2}{1458} \left(\frac{s^2(1+x\bar{y})}{c^2\bar{x}y} + \frac{c^2(1+x\bar{y})}{s^2\bar{x}y} \right) F(s_b, b), \\
\hat{T}_{c\sigma'\sigma'}^{+-} &= -\frac{\kappa_2}{729} \left(\frac{s^2(1+xy)}{c^2\bar{x}\bar{y}} + \frac{c^2(1+\bar{x}\bar{y})}{s^2xy} \right) J_0(-pb)F(s_c, b), \\
\hat{T}_{d\sigma'\sigma'}^{+-} &= -\frac{\kappa_2}{729} \left(\frac{s^2(1+\bar{x}\bar{y})}{c^2xy} + \frac{c^2(1+xy)}{s^2\bar{x}\bar{y}} \right) J_0(pb)F(s_d, b),
\end{aligned} \tag{46}$$

with the factor

$$\kappa_2 = \frac{\mu_\pi^2}{\omega^2} \kappa_1 = \frac{\mu_\pi^2}{\omega^2} \alpha \alpha_s(t_n) \pi^2 f_\pi^2. \tag{47}$$

Here J_0 is the Bessel function with the variable $pb(=2\omega s_c b)$ and the function $F(s_i, b)$ is defined as

$$F(s_i, b) = \begin{cases} 2\pi H_0^{(1)}(\sqrt{s_i}b) & \text{for } s_i > 0 \\ -4iK_0(\sqrt{-s_i}b) & \text{for } s_i < 0 \end{cases}. \tag{48}$$

The renormalization scales $t_n(n = a, b, c, d)$ entering \hat{T}_H as the arguments of strong coupling constant α_s , depend on the kinematics of the specific group which are chosen as

$$\begin{aligned}
t_a &= \max\{2\omega\sqrt{\bar{x}y}, 1/b\}, & t_b &= \max\{2\omega\sqrt{x\bar{y}}, 1/b\}, \\
t_c &= \max\{2\omega\sqrt{(s^2(\bar{x}-y)-\bar{x}\bar{y})}, 1/b\}, & t_d &= \max\{2\omega\sqrt{(s^2(x-\bar{y})-xy)}, 1/b\}.
\end{aligned} \tag{49}$$

The factors $s_n(n = a, b, c, d)$ come from the gluon propagators in each group

$$\begin{aligned}
s_a &= 4\bar{x}y\omega^2, & s_b &= 4x\bar{y}\omega^2, \\
s_c &= 4(\bar{x}-s^2)(y-c^2)\omega^2, & s_d &= 4(x-s^2)(\bar{y}-c^2)\omega^2.
\end{aligned} \tag{50}$$

In addition, it is worth noticing the hard kernels with different helicity have the relations

$$\hat{T}_{nij}^{++} = \hat{T}_{nij}^{--}, \quad \hat{T}_{nij}^{+-} = \hat{T}_{nij}^{-+}. \tag{51}$$

The formulas for the $\gamma\gamma \rightarrow K^+K^-$ process can be obtained directly with the replacements of $e_d \rightarrow e_s, f_\pi \rightarrow f_K, \mu_\pi \rightarrow \mu_K$ in the hard kernels and $\phi^\pi(x) \rightarrow \phi^K(x)$ in the convolution.

III. NUMERICAL ANALYSIS

The numerical analysis is performed in this section. Here we adopt the electromagnetic coupling constant $\alpha = 1/137$ and the QCD running coupling constant

$$\alpha_s(\mu^2) = \frac{\pi}{\beta_1 \ln(\mu^2/\Lambda_{QCD}^2)}, \tag{52}$$

with the QCD scale $\Lambda_{QCD} = 0.2$ GeV and the interaction scale $\mu = \mu_R$, the parameter $\beta_1 = (33 - 2N_f)/12$ with the number of quark flavors $N_f = 4$. The decay constants are taken as $f_\pi = 0.132$ GeV and $f_K = 0.160$ GeV.

The most important parameter we focus on is the chiral enhancement parameter μ_π , which plays an important role in the twist-3 contributions to the $\gamma\gamma \rightarrow \pi^+\pi^-$ process. However, the uncertainty of μ_π which is defined in Eq. (6) with the current-quark masses is large, see Ref. [44] for detailed discussion. The chiral perturbation theory defines the constant $\mu_\pi(1 \text{ GeV}) = 1.6 \pm 0.2$ GeV [46] via the quark condensate. Ref. [52] gives the value $\mu_\pi(1 \text{ GeV}) = 1.3 \pm 0.4$ GeV by fitting the transition form factor and the electromagnetic form factor to the available ‘‘world data’’ for the pion. In the intermediate energy, the author of Ref. [39] pointed out that μ_π is usually taken to be slightly lower $\approx 1.3 - 1.5$ GeV which is consistent with the fits to $B \rightarrow \pi$ transition form factor and the moment calculation applying QCD sum rule. In this work, we prefer using

$\mu_\pi(1 \text{ GeV}) = 1.4 \text{ GeV}$ [60], which is a reasonable value on all accounts, and following Ref. [52], we take the approximation $\mu_\pi \approx \mu_K$. Besides, the parameter μ_π evolves as

$$\mu_\pi(\mu^2) = L^{-1/\beta_1} \mu_\pi(\mu_0^2), \quad (53)$$

with

$$L = \frac{\alpha_s(\mu^2)}{\alpha_s(\mu_0^2)} = \frac{\ln(\mu_0^2/\Lambda_{QCD}^2)}{\ln(\mu^2/\Lambda_{QCD}^2)}. \quad (54)$$

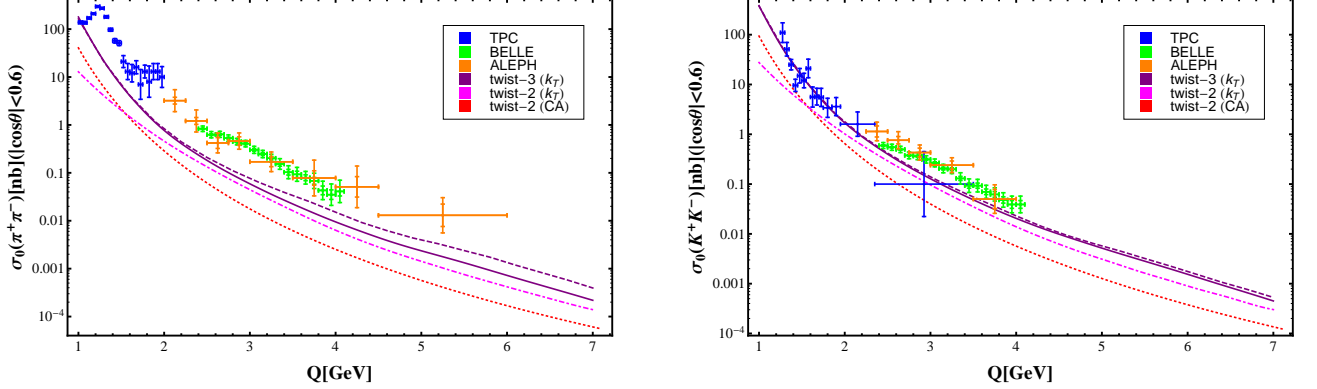


FIG. 2. Cross sections for $\gamma\gamma \rightarrow \pi^+\pi^-$, K^+K^- in the c.m. angular region $|\cos\theta| < 0.6$. Red dotted lines: the twist-2 results in the collinear approximation (CA); Magenta dot-dashed lines: the twist-2 results in the modified perturbative QCD approach (k_T); Purple solid lines: the results with the asymptotic twist-3 distribution amplitudes (as given in Eq. (19)); Purple dashed lines: the results with the nonasymptotic twist-3 distribution amplitudes [46, 48].

Then we perform the numerical analysis of the cross sections for the processes $\gamma\gamma \rightarrow \pi^+\pi^-$ and $\gamma\gamma \rightarrow K^+K^-$ in the c.m. angular region $|\cos\theta| < 0.6$. The predictions of the modified perturbative QCD approach for the cross section and its Q dependence are illustrated in Fig. 2. Including the high twists contributions, the comparisons of our theoretical predictions with the experimental data from TPC [19], BELLE [21] and ALEPH [20] are shown in this figure. From Fig. 2, one can obtain the following points:

- (1) For the twist-2 case, our new results (magenta dot-dashed lines) within the modified perturbative QCD approach improve the old ones (red dotted lines) within the collinear approximation, especially for the behavior of $Q < 2 \text{ GeV}$ regions. As it is seen, the cross sections for the collinear approximation at twist-2 level are significantly below the data, but our new results are less than an order of magnitude with the experimental data now. Rough estimation suggests 130% enhancement in the twist-2 parts between the collinear approximate and the modified perturbative QCD approach among the energy range of BELLE Collaboration.
- (2) For the twist-3 case, which we called twist-3 contributions generally refer to the ones including the twist-2 contributions, the cross sections obtained in the modified perturbative QCD approach are further improved. The difference between the solid and the dashed lines comes from the choice of the twist-3 distribution amplitudes, the former with the asymptotic forms (as indicated in Eq. (19)) and the latter with considering the QCD evolution of the distribution amplitudes [46, 48]. A 30% enhancement occurs between the twist-2 parts and the twist-3 parts (asymptotic forms) in the modified perturbative QCD approach among the BELLE range based on rough estimation. It is clear that the numerical results of the perturbative calculations are improved definitely in the modified perturbative QCD approach, and both the intrinsic transverse momenta and the high-twist contributions are considerable in the few GeV energy region.
- (3) A more detailed investigation has shown that the twist-3 corrections fall off rapidly with increasing Q and, beyond 10 GeV region both for pion and kaon case, fall below the twist-2 contributions. As is known that, the twist-2 contributions are expected to dominate in the cross section at the asymptotically large momentum transfers. However, as evident from Fig. 2, the higher twist contributions should be taken into account for the moderate energy regions.

Next we focus on the Q dependence of the cross section. As is known that the parametrization about the Q dependence of the cross section has the form $\sigma(\gamma\gamma \rightarrow M^+M^-) \propto Q^{-n_M}$. The results obtained by BELLE Collaboration [21] give $n_\pi = 7.9 \pm 0.4 \pm 1.5$ and $n_K = 7.3 \pm 0.3 \pm 1.5$ for $3.0 \text{ GeV} < Q < 4.1 \text{ GeV}$. On the other hand, Brodsky predicted a Q^{-6} dependence [3] of the cross section. The next-to-leading order (NLO) predictions [11] take the values $n_\pi = n_K = 6.9(7.4)$

for $\mu_R^2 = Q^2(Q^2/15)$. We also obtain $n_\pi = 7.29$ and $n_K = 7.32$ as well as $n_\pi = 4.55$ and $n_K = 4.50$ for the collinear approximation and the modified perturbative QCD approach at twist-2 level respectively, $n_\pi = 8.13$ and $n_K = 8.09$ as well as $n_\pi = 7.90$ and $n_K = 8.01$ for the asymptotic and nonasymptotic forms of distribution amplitudes at the twist-3 level in the modified perturbative approach respectively. The **FindFit** commands are applied to the energy region among 1 ~ 7 GeV. From the above discussion, it can be found that the modified perturbative QCD approach provides the different trends among 1~2 GeV region and our predictions particularly including the twist-3 contributions are in good agreement with the BELLE data as well as consistent with its tendency.

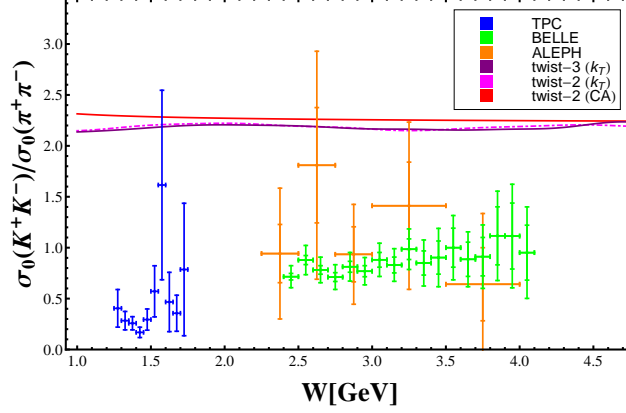


FIG. 3. Cross section ratio. Red solid line: the ratio in the collinear approximation (CA) for twist-2 case; Magenta dot-dashed line: the ratio in the modified perturbative QCD approach (k_T) for twist-2 case; Purple solid line: the ratio in the modified perturbative QCD approach for twist-3 case with the asymptotic distribution amplitudes. The experimental points are obtained from the data of Refs. [19–21].

For the ratio of kaon to pion cross section $\sigma_0(\gamma\gamma \rightarrow K^+K^-)/\sigma_0(\gamma\gamma \rightarrow \pi^+\pi^-)$ shown in Fig. 3, our predictions are close to 2.25 (red solid line) in the collinear approximation and 2.18 (magenta dot-dashed line) in the modified perturbative QCD approach for the twist-2 case as well as 2.16 (purple solid line) in the modified perturbative QCD approach for the asymptotic twist-3 case, and are similar with the Brodsky-Lepage prediction [3] and the NLO prediction [11], which are equal to $f_K^4/f_\pi^4 = 2.23$. While the BELLE results [21] give $0.89 \pm 0.04 \pm 0.15$ for $3.0 \text{ GeV} < Q < 4.1 \text{ GeV}$.

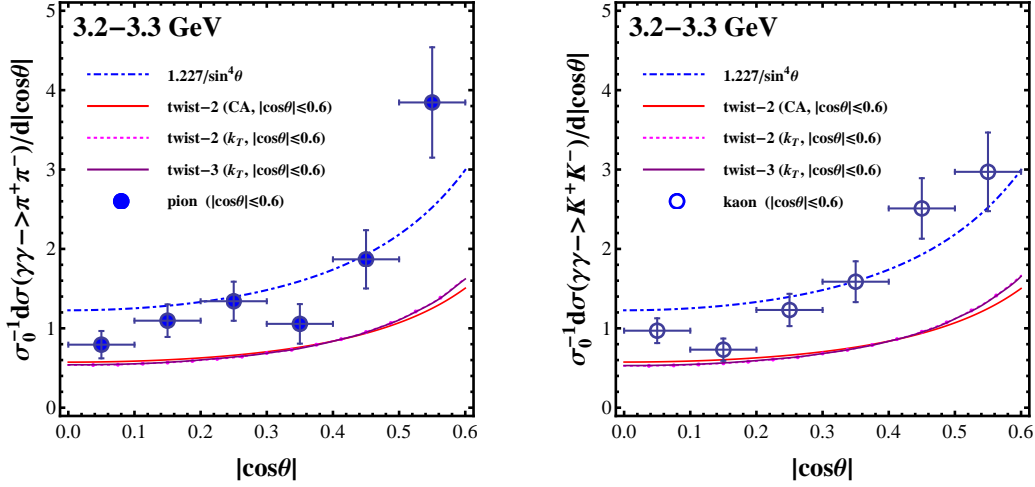


FIG. 4. Angular dependence of the cross section, $\sigma_0^{-1} d\sigma/d|\cos\theta|$, for the $\pi^+\pi^-$ (closed circles) and K^+K^- (open circles) processes. The notes of the lines are same as those in the caption of Fig. 3. The experimental points are from Ref. [21].

Fig. 4 shows the angular dependence of the cross section, $\sigma_0^{-1} d\sigma/d|\cos\theta|$, for the $\pi^+\pi^-$ and K^+K^- processes. The experimental points are obtained from BELLE Collaboration [21]. The blue dot-dashed line corresponds to $1.227/\sin^4\theta$ as the expectation behavior predicted by Brodsky-Lepage [3]. Fig. 4 shows the results for $Q = 3.2 - 3.3 \text{ GeV}$ which is in the middle of the BELLE range. We find that the results both for the twist-2 case and the twist-3 case are slightly dependent on $\cos\theta$ for a fixed Q and differ from the experiment data. The reason may be relate to the hierarchy $s^2 x \omega^2, s^2 \bar{y} \omega^2 \gg \bar{x} y \omega^2, \mathbf{k}_\perp^2$, which is

no longer operative at some values of the scattering angle. In the range of $1 \text{ GeV} < W < 7 \text{ GeV}$, a similar conclusion can be obtained.

IV. CONCLUSION

Our work represents the first investigation of higher-twist effects of the typical two-photon processes $\gamma\gamma \rightarrow \pi^+\pi^-, K^+K^-$ in the modified perturbative QCD approach, in which the intrinsic transverse momentum and Sudakov corrections are taken into account. We use the twist-2 and twist-3 light-cone wave functions incorporating transverse degrees of freedom as the nonperturbative dynamical inputs. The endpoint contribution can be effectively suppressed by the Sudakov factor $\exp[-S]$ and the threshold resummation factor $S_t(x)$. Through the above operations, the perturbative QCD calculation is more self-consistent and applicable. Our results for the cross section with twist-3 corrections agree well with the experimental data, and it seems that both the intrinsic transverse momentum and the higher-twist effects play a significant role in the few GeV region. Our next steps may be possible in two directions: the more appropriate choice of the meson distribution amplitudes and the more mature technology of the Fourier transformation of hard amplitudes.

In conclusion, we hope more works can be devoted to this subject both on theoretical and experimental sides and push forward our knowledge on the meson distribution amplitudes and perturbation mechanism to the exclusive processes.

ACKNOWLEDGMENTS

C. Wang would like to thank Ya-Dong Yang for valuable discussions and the English language revision.

Appendix A: The Sudakov function $s(\xi, b, Q)$

The expression of the Sudakov function $s(\xi, b, Q)$ appearing in Eq. (30) has the form [30, 55]:

$$s(\xi, b, Q) = \frac{A^{(1)}}{2\beta_1} \hat{q} \ln\left(\frac{\hat{q}}{\hat{b}}\right) + \frac{A^{(2)}}{4\beta_1^2} \left(\frac{\hat{q}}{\hat{b}} - 1\right) - \frac{A^{(1)}}{2\beta_1} (\hat{q} - \hat{b}) - \frac{A^{(1)}\beta_2}{4\beta_1^3} \hat{q} \left[\frac{\ln(2\hat{b}) + 1}{\hat{b}} - \frac{\ln(2\hat{q}) + 1}{\hat{q}} \right] \\ - \left[\frac{A^{(2)}}{4\beta_1^2} - \frac{A^{(1)}}{4\beta_1} \ln\left(\frac{e^{2\gamma-1}}{2}\right) \right] \ln\left(\frac{\hat{q}}{\hat{b}}\right) + \frac{A^{(1)}\beta_2}{8\beta_1^3} [\ln^2(2\hat{q}) - \ln^2(2\hat{b})], \quad (\text{A1})$$

with the variables

$$\hat{q} \equiv \ln\left(\frac{\xi Q}{\sqrt{2}\Lambda_{QCD}}\right), \quad \hat{b} \equiv \ln\left(\frac{1}{b\Lambda_{QCD}}\right), \quad (\text{A2})$$

and the coefficients $A^{(i)}$ and β_i

$$\beta_1 = \frac{33 - 2n_f}{12}, \quad \beta_2 = \frac{153 - 19n_f}{24}, \\ A^{(1)} = \frac{4}{3}, \quad A^{(2)} = \frac{67}{9} - \frac{\pi^2}{3} - \frac{10}{27}n_f + \frac{8}{3}\beta_1 \ln\left(\frac{e^\gamma}{2}\right), \quad (\text{A3})$$

where the number of quark flavors is $n_f = 4$ and γ is the Euler constant.

On the physical picture, the longitudinal momentum should be larger than the transverse momentum. It means that the function $s(\xi, b, Q)$ is defined for $\hat{q} > \hat{b}$ (i.e., $\xi Q/\sqrt{2} > 1/b$) and set to zero for $\hat{q} \leq \hat{b}$. The range of validity of Eq. (A1) for the Sudakov function is limited to not too small values for the transverse separation of quark and antiquark in the meson. Whenever $b \leq \sqrt{2}/\xi Q$ (i.e., $\hat{b} \geq \hat{q}$), the gluonic corrections are considered as higher-order corrections and absorbed in the hard scattering amplitude, hence they are not contained in the Sudakov factor. Moreover, the complete Sudakov factor $\exp[-S]$ is set to unity, if $\exp[-S] > 1$, which is the case in the small b region. As b increases the Sudakov factor $\exp[-S]$ decreases, reaching zero at $b = 1/\Lambda_{QCD}$. For b larger than $1/\Lambda_{QCD}$, the true soft region, the Sudakov factor is zero.

-
- [1] A. V. Efremov and A. V. Radyushkin, *Theor. Math. Phys.* **42**, 97 (1980), [*Teor. Mat. Fiz.*42,147(1980)].
- [2] G. P. Lepage and S. J. Brodsky, *Phys. Rev.* **D22**, 2157 (1980).
- [3] S. J. Brodsky and G. P. Lepage, *Phys. Rev.* **D24**, 1808 (1981).
- [4] V. L. Chernyak and A. R. Zhitnitsky, *Phys. Rept.* **112**, 173 (1984).
- [5] S. J. Brodsky, *AIP Conf. Proc.* **571**, 315 (2001), arXiv:hep-ph/0010176.
- [6] S. J. Brodsky, *Int. J. Mod. Phys.* **A30**, 1530014 (2015).
- [7] S. J. Brodsky, *Acta Phys. Polon.* **B37**, 619 (2006).
- [8] V. L. Chernyak, in *QCD in two photon process Taipei, Taiwan, October 2-4, 2012* (2012), arXiv:1212.1304.
- [9] V. L. Chernyak and S. I. Eidelman, *Prog. Part. Nucl. Phys.* **80**, 1 (2014), arXiv:1409.3348.
- [10] B. Nižić, *Phys. Rev.* **D35**, 80 (1987).
- [11] G. Duplanžić and B. Nižić, *Phys. Rev. Lett.* **97**, 142003 (2006), arXiv:hep-ph/0607069.
- [12] C. Vogt, in *QCD: Perturbative or nonperturbative? Proceedings, 17th Autumn School, Lisbon, Portugal, September 29-October 4, 1999* (1999), pp. 479–484, arXiv:hep-ph/9911253, URL <http://www.slac.stanford.edu/spires/find/books/www?cl=QCD161:A85:1999>.
- [13] C. Vogt, *AIP Conf. Proc.* **571**, 345 (2001), arXiv:hep-ph/0010040.
- [14] R.-C. Hsieh and H.-n. Li, *Phys. Rev.* **D70**, 056002 (2004), arXiv:hep-ph/0404109.
- [15] M. Diehl, P. Kroll, and C. Vogt, *Phys. Lett.* **B532**, 99 (2002), arXiv:hep-ph/0112274.
- [16] C. Vogt, *Nucl. Phys.* **A711**, 215 (2002), [,239(2002)], arXiv:hep-ph/0207077.
- [17] P. Kroll, *EPJ Web Conf.* **37**, 01019 (2012), arXiv:1209.1230.
- [18] N. Kivel (2013), arXiv:1307.0394.
- [19] H. Aihara et al. (TPC/Two Gamma), *Phys. Rev. Lett.* **57**, 404 (1986), URL <https://hepdata.net/record/ins228072>.
- [20] A. Heister et al. (ALEPH), *Phys. Lett.* **B569**, 140 (2003), URL <https://hepdata.net/record/ins626022>.
- [21] H. Nakazawa et al. (Belle), *Phys. Lett.* **B615**, 39 (2005), arXiv:hep-ex/0412058, URL <https://hepdata.net/record/ins667712>.
- [22] T. Mori et al. (Belle), *J. Phys. Soc. Jap.* **76**, 074102 (2007), arXiv:0704.3538.
- [23] S. Uehara et al. (Belle), *Phys. Rev.* **D78**, 052004 (2008), arXiv:0805.3387.
- [24] S. Uehara et al. (Belle), *Phys. Rev.* **D79**, 052009 (2009), arXiv:0903.3697.
- [25] K. Abe et al. (Belle), *Eur. Phys. J.* **C32**, 323 (2003), arXiv:hep-ex/0309077.
- [26] W. T. Chen et al. (Belle), *Phys. Lett.* **B651**, 15 (2007), arXiv:hep-ex/0609042.
- [27] S. Uehara et al. (Belle), *PTEP* **2013**, 123C01 (2013), arXiv:1307.7457.
- [28] C. Wang, M.-Z. Zhou, and H. Chen, *Eur. Phys. J.* **C77**, 219 (2017), arXiv:1512.04381.
- [29] J. Botts and G. F. Sterman, *Nucl. Phys.* **B325**, 62 (1989).
- [30] H.-n. Li and G. F. Sterman, *Nucl. Phys.* **B381**, 129 (1992).
- [31] C. Corianò, H.-n. Li, and C. Savkli, *JHEP* **07**, 008 (1998), arXiv:hep-ph/9805406.
- [32] R. Jakob and P. Kroll, *Phys. Lett.* **B315**, 463 (1993), [Erratum: *Phys. Lett.*B319,545(1993)], arXiv:hep-ph/9306259.
- [33] F.-g. Cao, Y.-b. Dai, and C.-s. Huang, *Eur. Phys. J.* **C11**, 501 (1999), arXiv:hep-ph/9711203.
- [34] S. Cheng and Z.-J. Xiao, *Phys. Lett.* **B749**, 1 (2015), arXiv:1505.02909.
- [35] J. Bolz, P. Kroll, and G. A. Schuler, *Eur. Phys. J.* **C2**, 705 (1998), arXiv:hep-ph/9704378.
- [36] H.-n. Li and H.-L. Yu, *Phys. Rev.* **D53**, 2480 (1996), arXiv:hep-ph/9411308.
- [37] Z.-T. Wei and M.-Z. Yang, *Nucl. Phys.* **B642**, 263 (2002), arXiv:hep-ph/0202018.
- [38] T. Kurimoto, H.-n. Li, and A. I. Sanda, *Phys. Rev.* **D65**, 014007 (2002), arXiv:hep-ph/0105003.
- [39] J.-W. Chen, H. Kohyama, K. Ohnishi, U. Raha, and Y.-L. Shen, *Phys. Lett.* **B693**, 102 (2010), arXiv:0908.2973.
- [40] U. Raha and H. Kohyama, *Phys. Rev.* **D82**, 114012 (2010), arXiv:1005.1673.
- [41] V. M. Braun and I. E. Filyanov, *Z. Phys.* **C44**, 157 (1989), [*Yad. Fiz.*50,818(1989)].
- [42] V. M. Braun and I. E. Filyanov, *Z. Phys.* **C48**, 239 (1990), [*Yad. Fiz.*52,199(1990)].
- [43] M. Beneke and T. Feldmann, *Nucl. Phys.* **B592**, 3 (2001), arXiv:hep-ph/0008255.
- [44] P. Kroll and K. Passek-Kumerički, *Phys. Rev.* **D97**, 074023 (2018), arXiv:1802.06597.
- [45] J. Bolz, P. Kroll, and G. A. Schuler, *Phys. Lett.* **B392**, 198 (1997), arXiv:hep-ph/9610265.
- [46] P. Ball, *JHEP* **01**, 010 (1999), arXiv:hep-ph/9812375.
- [47] P. Ball, V. M. Braun, and A. Lenz, *JHEP* **05**, 004 (2006), arXiv:hep-ph/0603063.
- [48] P. Ball and R. Zwicky, *Phys. Rev.* **D71**, 014015 (2005), arXiv:hep-ph/0406232.
- [49] V. M. Braun et al., *Phys. Rev.* **D74**, 074501 (2006), arXiv:hep-lat/0606012.
- [50] R. Arthur, P. A. Boyle, D. Brommel, M. A. Donnellan, J. M. Flynn, A. Juttner, T. D. Rae, and C. T. C. Sachrajda, *Phys. Rev.* **D83**, 074505 (2011), arXiv:1011.5906.
- [51] V. M. Braun, S. Collins, M. Göckeler, P. Pérez-Rubio, A. Schäfer, R. W. Schiel, and A. Sternbeck, *Phys. Rev.* **D92**, 014504 (2015), arXiv:1503.03656.
- [52] U. Raha and A. Aste, *Phys. Rev.* **D79**, 034015 (2009), arXiv:0809.1359.
- [53] P. Kroll, *Eur. Phys. J.* **C71**, 1623 (2011), arXiv:1012.3542.
- [54] H.-C. Hu and H.-n. Li, *Phys. Lett.* **B718**, 1351 (2013), arXiv:1204.6708.
- [55] M. Dahm, R. Jakob, and P. Kroll, *Z. Phys.* **C68**, 595 (1995), arXiv:hep-ph/9503418.
- [56] H.-n. Li, *Phys. Rev.* **D66**, 094010 (2002), arXiv:hep-ph/0102013.

- [57] H.-n. Li and S. Mishima, Phys. Rev. **D80**, 074024 (2009), arXiv:0907.0166.
- [58] C.-D. Lü, W. Wang, Y. Xing, and Q.-A. Zhang, Phys. Rev. **D97**, 114016 (2018), arXiv:1802.09718.
- [59] H.-n. Li, Y.-L. Shen, Y.-M. Wang, and H. Zou, Phys. Rev. **D83**, 054029 (2011), arXiv:1012.4098.
- [60] X. Liu, H.-n. Li, and Z.-J. Xiao, Phys. Rev. **D97**, 113001 (2018), arXiv:1801.06145.